Arabian Journal of Chemistry (2020) 13, 3210–3217

King Saud University

Arabian Journal of Chemistry

www.ksu.edu.sa
www.sciencedirect.com

ORIGINAL ARTICLE

Mechanical properties of carbon black/poly (ε-caprolactone)-based tissue scaffolds

Nuha Al Habis [a,*], Ahmed El Moumen [b], Mostapha Tarfaoui [b], Khalid Lafdi [a]

[a] University of Dayton, Dayton, OH 45469, United States
[b] ENSTA Bretagne, FRE CNRS 3744, IRDL, F-29200 Brest, France

Received 16 April 2018; accepted 21 October 2018
Available online 27 October 2018

KEYWORDS

Carbon black/poly(ε-caprolactone) nanocomposites;
Tissue scaffolds;
Computational homogenization;
Numerical approaches;
Microstructure

Abstract Carbon black (CB) spherical particles were added to poly(ε-caprolactone) (PCL) polymer to produce strong synthetic tissue scaffolds for biomedical applications. The objective of this paper is to study the mechanical behavior of CB/PCL-based nanocomposites using experimental tests, multi-scale numerical approaches, and analytical models. The mechanical properties of CB/PCL scaffolds were characterized using thermal mechanical analysis and results show a significant increase of the elastic modulus with increasing nanofiller concentration up to 7 wt%. Conversely, finite element computations were performed using a simulated microstructure, and a numerical model based on the representative volume element (RVE) was generated. Thereafter, Young's moduli were computed using a 3D numerical homogenization technique. The approach takes into consideration CB particles' diameters, as well as their random distribution and agglomerations into PCL. Experimental results were compared with data obtained using numerical approaches and analytical models. Consistency in the results was observed, especially in the case of lower CB fractions.

1. Introduction

The research over several decades has found that an increase in polymer mechanical properties is observed simultaneously with an increase in carbon nano-additive content (Al-Saleh and Sundararaj, 2011; Bortz et al., 2011). Fracture resistance of carbon nanofiber (CNF)/epoxy composites increased 66% and 78% as a result of the addition of 0.5 and 1.0 wt% CNF, respectively (Bortz et al., 2011). An increase in microhardness of CNF composites correlated with increasing CNF content when using the mixing method. The results showed that epoxy matrix microhardness increased by 53% (at 0.5 wt % CNF), 62% (at 0.75 wt% CNF) and 100% (at 1.0 wt% CNF). The high modulus strength and high aspect ratio of CNF was responsible for hardness enhancement (Bal, 2010).

Carbon nano-additives can be incorporated in medical applications efficiently. For instance, nanofibers are practical for neural tissue engineering because they allow the necessary mechanical support for nerve regeneration scaffolds, while simultaneously inhibiting non-neural cell growth. The scars which are caused by non-neural cell growth, are depressed by CNTs, meaning that CNTs lower the risk of scar tissue for-

* Corresponding author.
E-mail address: alhabisn1@gmail.com (N. Al Habis).
Peer review under responsibility of King Saud University.

Production and hosting by Elsevier

https://doi.org/10.1016/j.arabjc.2018.10.005
1878-5352

mation (Huang et al., 2006). To boost the mechanical properties of scaffolds, fiber size and nano-composition should be optimized. Research reported that bending Young's modulus increases as the fiber diameter of polymeric nanofibers decreases. Furthermore, the type of nanofiber materials, whether single materials or composite, can affect the mechanical properties. Biljana et al. posited that the nanofibers based on polyvinyl alcohol (PVA) and polyethylene oxide (PEO) demonstrated increase in elasticity with the reduction in bending Young's modulus. The increased elasticity is a property needed for wound and skin repairs. However, nanofiber-based on polyethylene oxide/chitosan (PEO 400 K/CS) is stiffer which consequently makes it a suitable candidate for bone, tendon, and cartilage tissue scaffold engineering (Janković et al., 2013). Cartilage tissue engineering has been used to develop polymer substrates with PLA nanofibers that had been modified with carbon nanotubes (CNTs) and gelatin (GEL). When comparing pure PLA, PLA + GEL, and PLA + CNTs, it has been found that PLA + CNTs demonstrated the highest values for tensile strength and Young's modulus as shown in Table 1. The results demonstrated a promising potential for tissue engineered scaffolds to be successfully used for repairing cartilages (Markowski et al., 2015).

Characterization of scaffold composites can also be made by means of analytical and numerical methods. Analytical methods can be divided into three groups including the well-known Voigt and Reuss (VR) bounds, Hashin and Shtrikman's bounds (Hashin et al., 1963), and third order bounds (Beran et al., 1966), in order to bound the properties and direct estimations of Mori-Tanaka's theory. The objective of the mechanics of microstructures is to derive the physical properties and the local fields and deformation of composite specimens from the knowledge of the nature of the constituents, their distribution, and their constitutive laws. Bergström et al. (1998) modeled the CB aggregates as squares or dodecaedrons in an elastomeric matrix and as the union of CB spherical-shaped particles by Naito et al. (2007). A composite model was also obtained from periodic homogenization by placing a spherical CB particle at the center of a tetrakaidecahedron cell (Laiariandrasana et al., 2009). A 3D morphological model was used by Jean et al. (2011a) in order to estimate the effective elastic modulus of a polymer matrix with CB fillers based on large-scale finite element (FE) computations. The addition of CB to polymer leads to significant improvements of the physical and the mechanical properties of composites. Djebara et al. (2016) were interested in modeling the elastic modulus of polymer nanocomposites reinforced with rigid particles using numerical homogenization techniques based on the FE method. The elastic properties of the studied microstructure were obtained with different boundary conditions, which included the effect of particle concentration and their distributions. Several references were very relevant to the modeling approaches of CB filled polymer composites (Laiarinandrasana et al., 2012; Jean et al., 2011a; Omnès et al., 2008). All these published works have shown the need for a three-dimensional microstructural model that took into account the interaction between aggregates and the interaction of CB fillers with the polymer.

Table 1 Nanofibrous scaffolds with PLA (Markowski et al., 2015).

Type	Tensile Strength (MPa)	Young's Modulus (MPa)
PLA+CNT	8.8 ± 0.7	461 ± 39
PLA	1.8 ± 0.4	178 ± 14
PLA+GEL	6.2 ± 0.3	375 ± 22

In this paper, the effect of CB nano-additives on the mechanical properties of nanocomposite scaffolds was studied experimentally, analytically and numerically. The fraction of CB particles in the mixes varied from 0% to 10 wt%. The modeling methodology was based on a 3D numerical homogenization technique with the help of finite element analysis software, while the theory of bounds and direct estimations were carried out using the analytical approach. The 3D modeling took into account the three phases: the CB particles phase, the aggregates phase and the PCL matrix. The experimental, analytical and numerical results were compared for various CB concentrations.

2. Materials and experimental methods

2.1. Materials

Polycaprolactone (PCL), ($\overline{M}_w$ = 80,000) was purchased from Sigma Aldrich. Carbon black (CB) is Vulcan XC 72R, Cabot®. Scaffolds were prepared by mixing 14 wt% PCL with CB particles. Five different weight percentages of CB were dispersed in 5 ml of acetone and were ultra-sonicated for two days.

As shown in (Fig. 1), the morphology of the CB was characterized. Using dark field imaging, we can observe that CB consists of spherical nanoparticles in which the graphene layers are arranged in the form of onion like structure (Heidenreich et al., 1968). These particles have an average dimension of 300 nm.

2.2. Preparation of the film scaffolds

Scaffolds were prepared by mixing 14 wt% PCL with CB particles. Five different weight percentages of CB were dispersed in 5 ml of acetone and were ultra-sonicated for two days. Following the ultrasonication process, a solution of 0.644 g PCL and 5 ml acetone was stirred at a temperature of 65 °C for two hours. Then, a spin coater method (Speed line P2604 Technologies, see Fig. 2a) was used to produce a PCL/CB thin film scaffold using a Spin speed of 3000 rpm for 90 s. The dimension of the specimen is (4.85 mm width, 8 mm length) with 0.02 mm in thickness. The mechanical properties of all specimens were measured by a thermal mechanical analysis (TMA, Q400, TA universal), see Fig. 2b.

3. Results and discussion

A study of the mechanical properties is an important test of many field spatially biomedical applications. The mechanical properties can control the performance of the biomedical tool such as a scaffold. A scaffold based on CB can provide an excellent mechanical property more than a polymer scaffold. This work examined the mechanical behavior of different

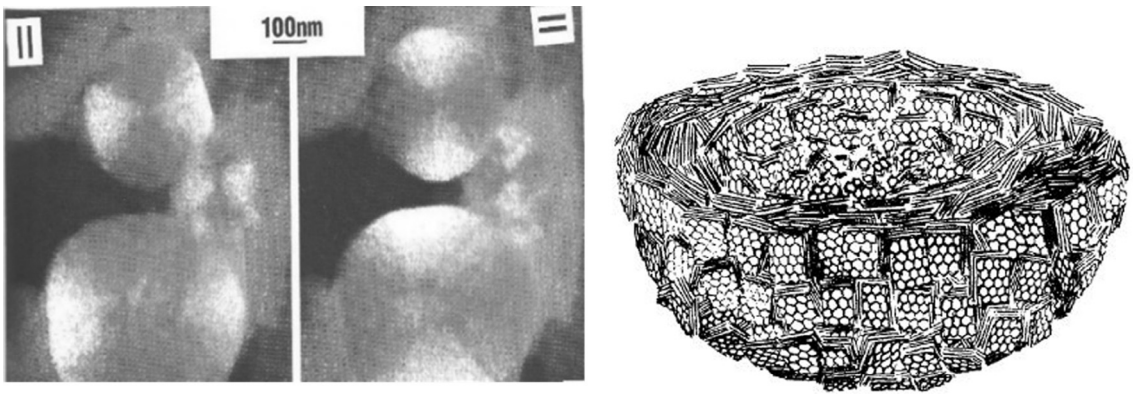

Fig. 1 Dark field imaging shows the onion-like structure of carbon black (Heidenreich et al., 1968).

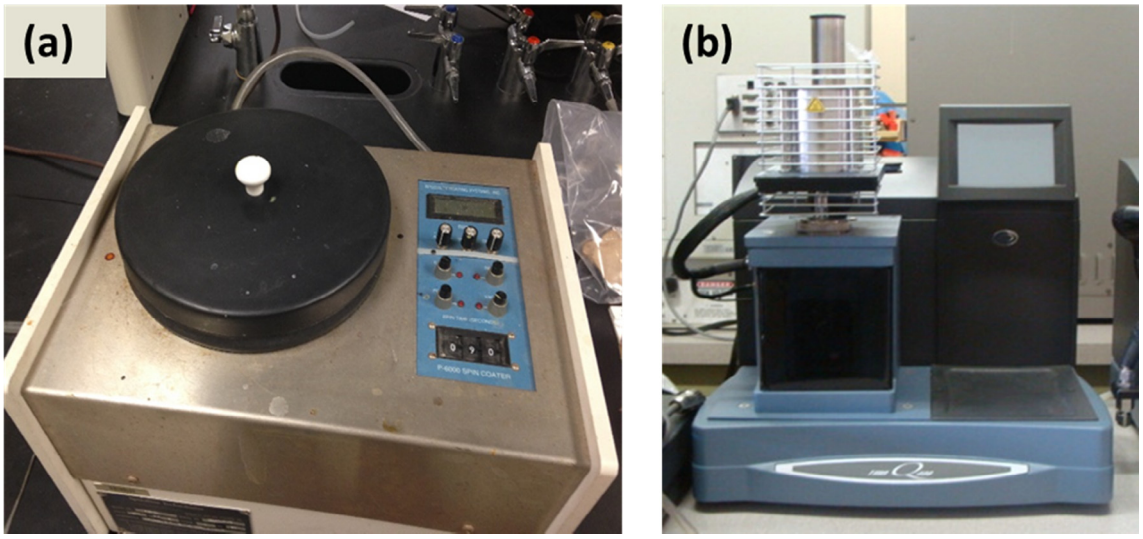

Fig. 2 Machine tests: (a) Spine coating device (b) Thermal mechanical analysis (TMA) device.

specimens of scaffold reinforced with CB rigid particles. (Fig. 3) shows the tensile stress curves of varieties of concentrations of CB thin film scaffolds. After comparing between distinct concentrations of CB additive with PCL, scaffold composites with 7% of concentration shows higher strength than other concentrations and pure PCL. In fact, an incorporation of minor amounts of CB (< 10% by weight) in polymer mixes improves the mechanical properties of the polymer composites.

Increasing CB nano-additives in the polymeric matrix showed an obvious enhancement in mechanical properties. The averaged Young's moduli and fracture were determined. These values correspond to the average Young's modulus for all tested specimens. Table 2 presented a measurement of modulus and ultimate stress of the scaffold as a function of CB additives concentration. The 7 wt% CB concentration has the highest mechanical properties, (101.25 MPa) for Young' modulus and (2.8 MPa) for ultimate stress, compared to other concentrations. The 10 wt% has the smallest averaged Young's modulus (58.7 MPa). (Fig. 4) showed the relationship of modulus versus additives concentration. After adding CB particles to the polymeric matrix an increase in the modulus value was observed until it reached the threshold of 7%wt concentration of additives, and then a decrease in the modulus occurred. With adding 7% of CB into composite scaffold, an almost 64% improvement in the Young's modulus was observed. Then, when the concentration changed from 7 and 10% a sharp decrease occurred (5.02% of reduction).

Once the experimental characterization of CB filled polymer composites was completed. A modelling study was resumed using two approaches: (1) an analytical modelling of CB/PCL using the existing analytical models and bounds and (2) a numerical homogenization of these samples using finite element method (FEM). We have focused on the multiscale analysis of the homogenized elastic moduli through knowledge acquired from the mechanical properties of each phase: CB, PCL and their distributions. The elastic properties of the PCL matrix were computed experimentally, and also for CB properties published data was used (Jean et al., 2011a). For CB particles, the Poisson ratio is usually taken as 0.3 and the Young's modulus is 80,000 MPa. A comparison was carried out between the experimental data and the obtained results from the analytical and numerical homogenization techniques.

3.1. Analytical modelling of CB/PCL elastic moduli

Various analytical homogenization methods can be found in the literature. A list of these models was presented by

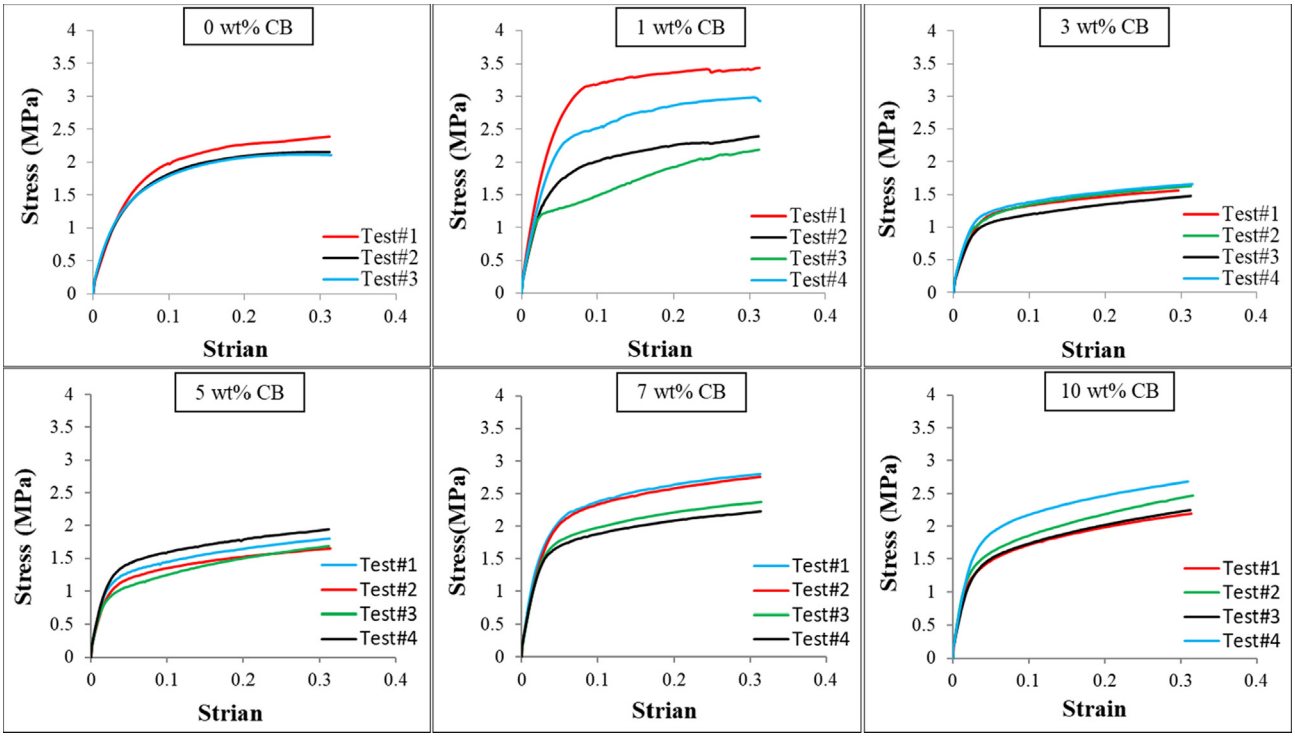

Fig. 3 Typical stress-strain curves for 0, 1, 3, 5, 7 and 10 wt% CB obtained during experimental testing on film scaffolds.

Table 2 Young's modulus and fracture of CB additive/PCL of composite scaffold.

CB (wt%)	Young's Moduli (MPa)	Standard Deviation	Gain (%)	Ultimate Stress (MPa)	Variation (%)
0	61.80	9.92	0	2.71	0
1	65.20	9.01	+5.50	2.74	+23.98
3	80.67	24.32	+30.54	1.58	−15.84
5	87.60	20.43	+40.75	1.77	−19.91
7	101.25	27.68	+63.83	2.54	+26.70
10	58.70	2.97	−5.02	2.40	+8.60

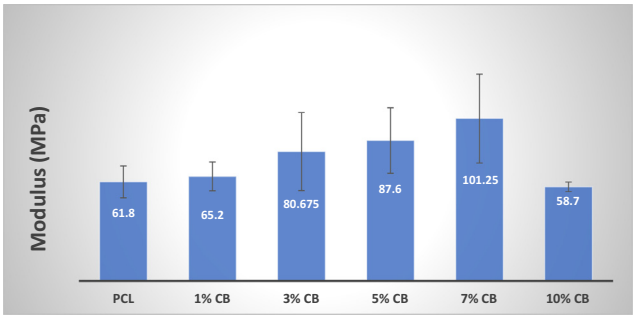

Fig. 4 The relationship of modulus vs. additives concentration for film scaffolds.

Buryachenko et al. (2007). The popular existing approaches will be assessed in the isotropic case namely: the Mori and Tanaka model (1973), the Smallwood (1944) and Guth-Gold (1938) models, the first-order bounds of Voigt and Reuss, the optimal bounds of Hashin and Shtrikman (1963), and the third order bounds (3OB) of Beran et al. (1966) and Milton (1981). Using these models, elastic properties of CB/PCL are determined by knowing those of each phase, "m: PCL matrix" and "i: CB inclusion", and "p" CB volume fraction. Mathematical expressions of each model are expressed and given by equations given in next sections.

3.1.1. Analytical bounds for CB/PCL modelling

The mechanical properties of composites can be bounded from physical information of the constituents. The more common bounds are Hashin and Shtrikman's (HS) based on the volume fraction of components and the third order bounds (3OB). In practice, it is difficult to obtain useful and exact results beyond the 3OB. The expressions of these bounds are:

- **Hashin Shtrikman (HS) bounds** (1963)

$$\begin{cases} k_{HS}^{-} = k_m + \dfrac{p}{1/(k_i-k_m)+3(1-p)/(3k_m+4\mu_m)} \\ k_{HS}^{+} = k_i + \dfrac{1-p}{1/(k_m-k_i)+3p/(3k_i+4\mu_i)} \end{cases} \quad (1)$$

$$\begin{cases} \mu_{HS}^{-} = \mu_m + \frac{p}{1/(\mu_i-\mu_m)+6(1-p)(k_m+2\mu_m)/5\mu_m(3k_m+4\mu_m)} \\ \mu_{HS}^{+} = \mu_i + \frac{1-p}{1/(\mu_m-\mu_i)+6p(k_i+2\mu_i)/5\mu_i(3k_i+4\mu_i)} \end{cases} \quad (2)$$

where μ the shear modulus, k the bulk modulus, the subscripts "m" and "i" denote matrix and particles phases, respectively, p the volume fraction of the CB particles and the symbol "+ and −" denotes upper and lower HS bounds.

- **Third order bounds (3OB)** (Beran et al., 1966; Milton, 1981).

3OB are the most sophisticated analytical models for estimations of elastic, thermal and electrical properties of spherical particle reinforced polymers. They depend on the properties of two phases, the filler volume fraction, the particle shape and their distribution and on the morphological function ζ which describe the distribution of CB particles. These bounds were initially proposed by Beran et al. (1966) and Milton (1981) and summarized by Toquato (1991). These bounds are valid for multiphase media, and more generally for elastic properties of random two-phase materials with overlapping spheres. The bounds are given in term of the moduli of phases and their volume fractions. Analytical expressions are highlighted and detailed in the book by Toquato (1991) and Jeulin et al. (2001).

HS and 3OB models obviously propose to calculate the bulk and shear moduli. It should be pointed out that to derive Young's modulus, Eq. (3) is used.

$$E = 9k\ \mu/(3k + \mu) \quad (3)$$

where E, μ and k are the Young's modulus, shear modulus and bulk modulus, respectively.

3.1.2. Direct analytical estimation

The direct analytical models, adapted for rigid spheres, used in this investigation were presented by Eqs. (4) and (5), respectively, represent the Smallwood (S) and Guth-Gold (GG) models (Smallwood, 1944; Guth et al., 1938). It is well known that Mori–Tanaka's model and the generalized self-consistent estimates (GSCE) (Christensen et al., 1979) cannot give a good prediction for the case of composites with CB particle agglomeration (Ma et al., 2004).

$$E_{Smallwood} = E_m(1 + 2.5p) \quad (4)$$

$$E_{Guth-Gold} = E_m(1 + 2.5p + 14.1p^2) \quad (5)$$

The evolution of the homogenized Young's modulus vs. CB fractions was studied. Table 3 illustrates the comparison between analytical models and the experiment data for CB fractions ranging from 0% to 10%.

For different concentrations of CB aggregates, it appears that the experimental Young's modulus values systematically lie between the HS and 3 PB bounds, which agrees with the homogenization theory. It also appears that for lower concentrations, existing analytical models closely match the experimental data including the HS+. Beyond a proportion of 10%, the experimental values decrease; this limit corresponds to the percolation threshold. Aside from the effect of aggregate size, the physico-chemical phenomena could be the cause of poor model estimation for large CB fractions.

Evaluations of the elastic properties of CB polymer composites can be obtained by means of several analytical methods. These models obviously converge when the volume fraction of particles or the contrast between the properties of phases is too small. Otherwise, a notable difference was observed. Note that, an alternative way of solving CB/PCL homogenization problems consists of applying numerical methods.

3.2. Numerical modelling of CB/PCL elastic moduli

Regarding the numerical techniques, the homogenization problem is solved using simulations on samples of microstructures for which the representative volume element (RVE) plays a key role. The RVE is defined as the volume of CB/PCL composite material that contains a sufficient number of CB particles.

3.2.1. Generating and meshing of CB/PCL model

To model the structure of a polymer with carbon black fillers, Jean et al. (2011b) presents various kinds of models adapted for this situation. According to Ma et al. (2004) only 27 CB particles randomly placed in a composite domain suffice to give an accurate prediction. Both studies of El Moumen et al. (2015a, 2013) and Beicha et al. (2016) show that a RVE of 50 rigid spheres is the volume minimum size necessary to give a realistic estimation. (Fig. 5a) shows microscopic morphology of CB-filled polymer matrix. Qualitatively, this morphology illustrates that the microstructure of CB/polymer contains three scales. These scales are: the scale of the PCL matrix, the scale of aggregates, and the scale of CB particles. In our study the CB spherical particles have a mean radius of 300 nm. The union of set particles creates aggregates. Looking at the morphology, it seems that the distribution of CB is homogeneous with some aggregates. To model with precision this microstructure, all of these morphological parameters are needed.

In our computation, 1000 CB particles are randomly implanted in PCL domain with the possibility of interpenetra-

Table 3 Confrontation of experimental data with different analytical models.

Mass fraction (%)	Volume fraction (%)	HS (MPa)	3OB- (MPa)	S (MPa)	GG (MPa)	Test (MPa)	3OB+ (MPa)	HS+ (MPa)
0	0	61.80	61.80	61.80	61.80	61.8 ± 9.92	61.80	61.80
1	0.60	62.53	62.60	62.73	62.76	65.2 ± 9.01	64.43	302.67
3	1.82	64.033	64.24	64.61	64.90	80.675 ± 24.30	81.27	795.68
5	3.06	65.59	65.97	66.53	67.34	87.6 ± 20.43	113.95	1302.92
7	4.32	67.23	67.77	68.47	70.10	101.25 ± 27.68	163.08	1824.93
10	6.25	69.80	70.66	71.45	74.86	58.7 ± 2.97	269.80	2637.68

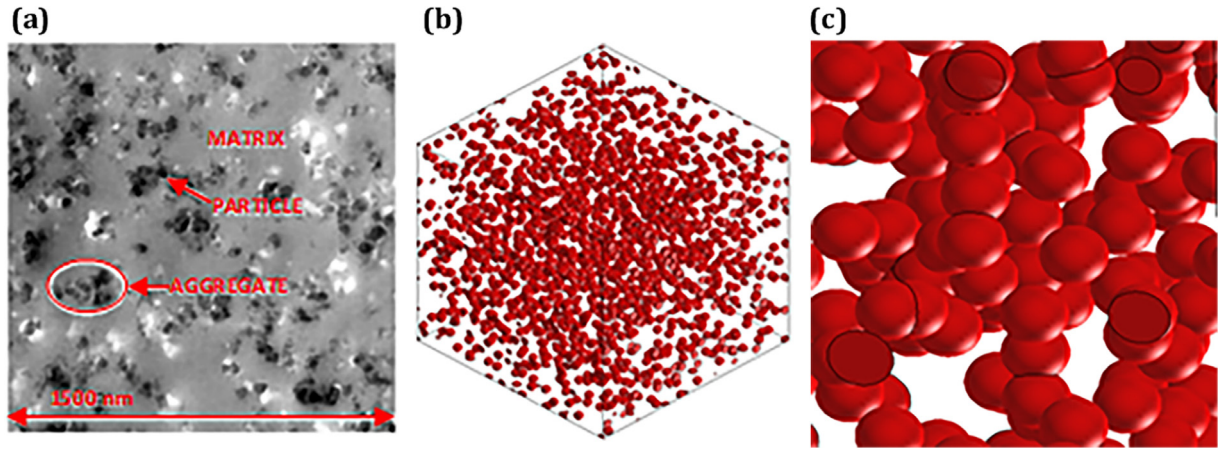

Fig. 5 Microstructures of CB/PCL composites. (a) CB randomly distributed in PCL polymer matrix (Ma et al., 2004), (b) Simulated microstructure with 1000 CB particles, (c) Zoom in on the aggregates phases.

tion of coating in order to create a clustering phase (or aggregates). Using a model with 27 CB spheres as proposed by Ma et al. (2004), no aggregates phase is observed. For that purpose, we have considered the volume with the maximum number of particles. The algorithm of implementation has already been described in our several works (El Moumen et al., 2015) and proposed by Digimat-FE software. (Fig. 5b) shows the microstructure of PCL containing 10% CB fillers. This RVE clearly reveals the multiscale microstructure of this composite with three scales: spherical particles, the aggregates phase, and the PCL matrix. A zoom out in the aggregate phase is presented in (Fig. 5c). This phase is obtained by overlapping spheres.

Several techniques are available to mesh a microstructure within the FE method. In the present work, priority has been given to create a FE mesh that follows the microstructure interfaces and constituents: particles, aggregates and a matrix. This is called the conforming meshing technique, (EL Moumen et al., 2015a; Jean et al., 2011a; Frey et al., 1999). Digimat-FE software is used with 324,133 tetrahedral elements taking into account internal coarsening and curvature control of aggregates. We have also defined how finely the curved edges are discretized by defining the chordal deviation ratio in the software. An example of meshed RVE is presented in (Fig. 6) for the PCL matrix, CB particles and PCL/CB scaffold composites.

3.2.2. Confrontation of experimental data with analytical and numerical approaches

A simple uniaxial test meant to adopt the periodic tension boundary conditions was applied to the generated microstructures of CB/PCL. The homogenized Young's modulus was determined with the help of FEM. The numerical results obtained for various particle concentrations were displayed in Table 4 and compared with experimental data and analytical models. As expected, these results increase when increasing the CB concentration and more closely match the experimental data for the case of lower fractions. The maximum difference between numerical and experimental results is found in the case of high CB fractions starting at 7%. But taking into account the standard deviation of experimental data, it appears that the results are consistent. Methods for estimating mechanical properties are based on the micromechanics interaction of composite constituents. In the case of CB scaffold composites, there is also a chemical interaction between the rigid particles and the PCL matrix. This chemical interaction does not take into account in analytical and numerical approaches. The difference between the numerical micro-

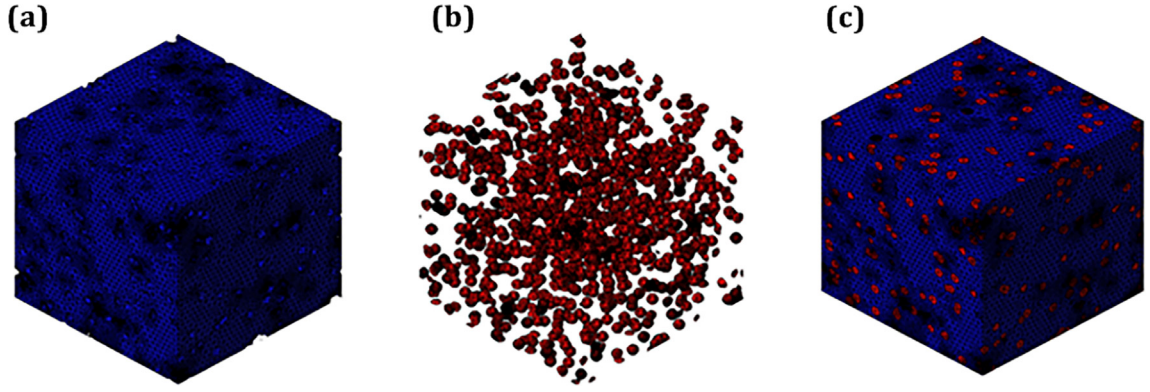

Fig. 6 Meshes of microstructures used for numerical simulations. (a) Only PCL matrix, (b) Only CB rigid spheres, (c) CB/PCL matrix.

Table 4 Homogenized Young's modulus: confrontation between experimental, numerical and analytical results.

Mass Fraction (%)	Volume Fraction (%)	HS- (MPa)	3OB- (MPa)	S (MPa)	GG (MPa)	FEA (MPa)	Test (MPa)	3OB + (MPa)	HS + (MPa)
0	0	61.80	61.80	61.80	61.80	61.80	61.8 ± 9.92	61.80	61.8
1	0.60	62.53	62.60	62.73	62.76	62.63	65.2 ± 9.01	64.43	302.67
3	1.82	64.03	64.24	64.61	64.90	64.42	80.675 ± 24.32	81.27	795.68
5	3.06	65.59	65.97	66.53	67.34	68.33	87.6 ± 20.43	113.95	1302.92
7	4.32	67.23	67.77	68.47	70.10	69.67	101.25 ± 27.68	163.08	1824.93
10	6.25	69.80	70.66	71.45	74.86	72.80	58.7 ± 2.97	269.80	2637.68

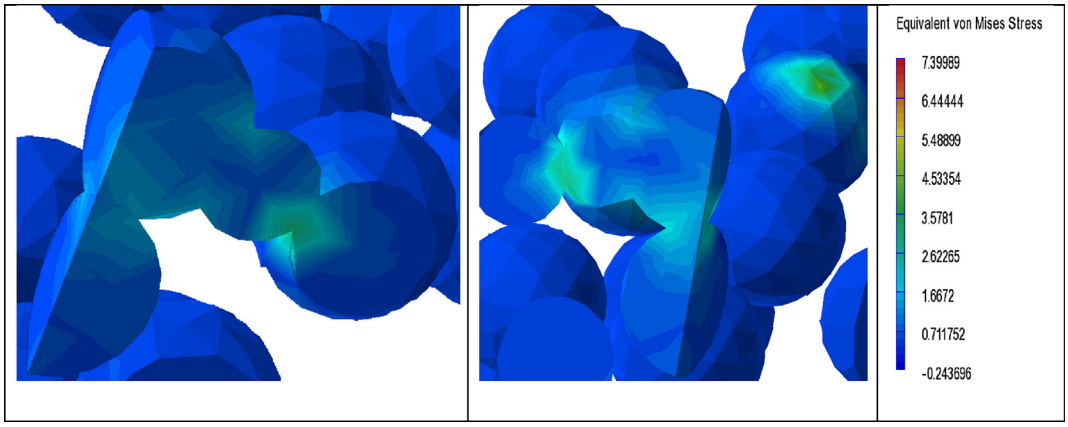

Fig. 7 Zoom on the aggregates zone of CB particles with distribution of stress.

scale homogenization and macroscopic experimental data can be justified by:

1. both of constituent's behavior in the numerical model were assumed to be linear while the polymer matrix behavior for example is visco-elastic,
2. experimental manufacturing process can affect the elastic moduli,
3. CB distribution is considered randomly in the homogenization models and some of them can be take cluster or aggregate distribution,
4. mesh resolution can also affect the properties and generates a small error, etc.
5. distribution of CB into nano-scale RVE differ from the experimental specimens.

This part indicates also that CB agglomeration generates the stress concentrations at the particle/matrix interface. In the case of high CB density, the numerical model shows a fundamental change in the profile of the interfacial stress (see Fig. 7). It is apparent that the distribution of stress is drastically changed in the presence of aggregates. In rigid particle-reinforced polymer composites, the onset of damage occurs at aggregate zone or near particle/polymer interfaces, where stress concentrations are the highest due to the property mismatch of the two materials properties. For that purpose, it is important to create a homogeneous distribution of the CB into scaffold composites, with minor aggregates, in order to redistribute the stresses at microscale and with it to change the mechanism of crack initiation.

4. Discussion and conclusion

Carbon black (CB) spherical particles were added to poly(ε-caprolactone) (PCL) polymer to produce strong synthetic tissue scaffolds for biomedical applications. The objective of this paper was to study the mechanical behavior of CB/PCL-based nanocomposites using experimental tests, multi-scale numerical approaches, and analytical models. The mechanical properties of CB/PCL scaffolds were characterized using thermal mechanical analysis and results show a significant increase in the elastic modulus with increasing carbon black concentration up to 7 wt%. This negative effect occurred because of the formation of aggregates. Carbon black's natural tendency for agglomeration in polymeric matrices consequently decreases the mechanical properties (Khodaverdi et al., 2014). This is a major problem because of stress concentration around the inclusions and areas with defects. Conversely, finite element computations were performed using simulated microstructure and a numerical model based on the representative volume element (RVE) that was generated. Thereafter, Young's moduli were computed using a 3D numerical homogenization technique. The approach takes into consideration, CB particles' lengths, their random distribution and agglomerations into PCL. Experimental results were compared with Data obtained

using numerical approaches and analytical models. Consistency was observed, especially in the case of lower CB fractions.

References

Al-Saleh, M.H., Sundararaj, U., 2011. Review of the mechanical properties of carbon nanofiber/polymer composites. Compos. A Appl. Sci. Manuf. 42 (12), 2126–2142.

Bal, S., 2010. Experimental study of mechanical and electrical properties of carbon nanofiber/epoxy composites. Mater. Des. (1980–2015) 31 (5), 2406–2413.

Beicha, D., Kanit, T., Brunet, Y., Imad, A., El Moumen, A., Khelfaoui, Y., 2016. Effective transverse elastic properties of unidirectional fiber reinforced composites. Mech. Mater. 102, 47–53.

Beran, M., Molyneux, J., 1966. Use of classical variational principles to determine bounds for the effective bulk modulus in heterogeneous media. Q. Appl. Math. 24 (2), 107–118.

Bergström, J.S., Boyce, M.C., 1998. Constitutive modeling of the large strain time-dependent behavior of elastomers. J. Mech. Phys. Solids 46 (5), 931–954.

Bortz, D.R., Merino, C., Martin-Gullon, I., 2011. Carbon nanofibers enhance the fracture toughness and fatigue performance of a structural epoxy system. Compos. Sci. Technol. 71 (1), 31–38.

Buryachenko, V., 2007. Micromechanics of Heterogeneous Materials. Springer Science & Business Media. ISBN:0387368272 9780387368276.

Christensen, R.M., Lo, K.H., 1979. Solutions for effective shear properties in three phase sphere and cylinder models. J. Mech. Phys. Solids 27 (4), 315–330.

Djebara, Y., El Moumen, A., Kanit, T., Madani, S., Imad, A., 2016. Modeling of the effect of particles size, particles distribution and particles number on mechanical properties of polymer-clay nanocomposites: numerical homogenization versus experimental results. Compos. B Eng. 86, 135–142.

El Moumen, A., Kanit, T., Imad, A., El Minor, H., 2015a. Effect of reinforcement shape on physical properties and representative volume element of particles-reinforced composites: statistical and numerical approaches. Mech. Mater. 83, 1–16.

El Moumen, A., Kanit, T., Imad, A., El Minor, H., 2015b. Computational thermal conductivity in porous materials using homogenization techniques: numerical and statistical approaches. Comput. Mater. Sci. 97, 148–158.

El Moumen, A., Kanit, T., Imad, A., Minor, H.E., 2013. Effect of overlapping inclusions on effective elastic properties of composites. Mech. Res. Commun. 53, 24–30.

Frey, P., Georges, P., 1999. Mesh Generation: Application to Finite Elements. HERMES, Paris.

Guth, E., Gold, O., 1938. On the hydrodynamical theory of the viscosity of suspensions. Phys. Rev. 53 (322), 2–15.

Hashin, Z., Shtrikman, S., 1963. A variational approach to the theory of the elastic behaviour of multiphase materials. J. Mech. Phys. Solids 11 (2), 127–140.

Heidenreich, R.D., Hess, W.M., Ban, L.L., 1968. A test object and criteria for high resolution electron microscopy. J. Appl. Crystallogr. 1 (1), 1–19.

Huang, Y.C., Huang, Y.Y., 2006. Tissue engineering for nerve repair. Biomed. Eng.: Appl. Basis Commun. 18 (03), 100–110.

Janković, B., Pelipenko, J., Škarabot, M., Muševič, I., Kristl, J., 2013. The design trend in tissue-engineering scaffolds based on nanomechanical properties of individual electrospun nanofibers. Int. J. Pharm. 455 (1), 338–347.

Jean, A., Willot, F., Cantournet, S., Forest, S., Jeulin, D., 2011a. Large scale computations of effective elastic properties of rubber with carbon black fillers. Int. J. Multiscale Comput. Eng. 9 (3), 271–303.

Jean, A., Jeulin, D., Forest, S., Cantournet, S., N'Guyen, F., 2011b. A multiscale microstructure model of carbon black distribution in rubber. J. Microsc. 241 (3), 243–260.

Jeulin, D., Ostoja-Starzewski, M. (Eds.), 2001. Mechanics of Random and Multiscale Microstructures. Springer, Wien-New York, pp. 33–91.

Khodaverdi, F., Hemati, M., Shekarian, E., Tarighaleslami, A.H., 2014. Morphology, thermal and mechanical properties of carbon black/high density polyethylene (CB/HDPE) composite. Adv. Environ. Biol. 8 (11), 1262–1265.

Laiarinandrasana, L., Jean, A., Jeulin, D. S., Forest, S., 2009. Modelling the effects of various contents of fillers on the relaxation rate of filled rubbers. In: Constitutive Models for Rubber VI. Proceedings of 6th European Conference on Consitutive Models for Rubber, ECCMR 2009, Dresden, Germany, 7–10 September 2009.

Laiarinandrasana, L., Jean, A., Jeulin, D., Forest, S., 2012. Modelling the effects of various contents of fillers on the relaxation rate of elastomers. Mater. Des. 33, 75–82.

Ma, H., Hu, G., Huang, Z., 2004. A micromechanical method for particulate composites with finite particle concentration. Mech. Mater. 36 (4), 359–368.

Markowski, J., Magiera, A., Lesiak, M., Sieron, A.L., Pilch, J., Blazewicz, S., 2015. Preparation and characterization of nanofibrous polymer scaffolds for cartilage tissue engineering. J. Nanomater. 16 (1), 45.

Milton, G.W., 1981. Bounds on the electromagnetic, elastic, and other properties of two-component composites. Phys. Rev. Lett. 46 (8), 542.

Mori, T., Tanaka, K., 1973. Average stress in matrix and average elastic energy of materials with misfitting inclusions. Acta Metall. 21 (5), 571–574.

Naito, M., Muraoka, K., Azuma, K., Tomita, Y., 2007. 3D modeling and simulation of micro to macroscopic deformation behavior of filled rubber. In: Boukamel, A., Laiarinandrasana, L.S.M., Verron, E. (Eds.), Constitutive Models for Rubber V. Proceedings of 5th European Conference on Consitutive Models for Rubber, ECCMR2007, Paris, France, 4–7 September 2007. Taylor and Francis, London, pp. 141–146.

Omnès, B., Thuillier, S., Pilvin, P., Grohens, Y., Gillet, S., 2008. Effective properties of carbon black filled natural rubber: experiments and modeling. Compos. A Appl. Sci. Manuf. 39 (7), 1141–1149.

Smallwood, H.M., 1944. Limiting law of the reinforcement of rubber. J. Appl. Phys. 15 (11), 758–766.

Torquato, S., 1991. Random heterogeneous media: microstructure and improved bounds on effective properties. Appl. Mech. Rev. 44 (2), 37–76.